

Controlled Formation of Optically Reflective and Electrically Conductive Silvered Surfaces on Polyimide Film via a Direct Ion-Exchange Self-Metallization Technique Using Silver Ammonia Complex Cation as the Precursor

Shengli Qi, Zhanpeng Wu, Dezhen Wu,* and Riguang Jin

State Key Laboratory of Chemical Resource Engineering, Beijing University of Chemical Technology, Beijing 100029, China

Received: December 2, 2007; In Final Form: February 15, 2008

Double-surface-silvered polyimide films have been successfully fabricated using silver ammonia complex cation ($[\text{Ag}(\text{NH}_3)_2]^+$) as the silver precursor and 3,3',4,4'-benzophenonetetracarboxylic dianhydride/4,4'-oxidianiline- (BTDA/ODA-) based poly(amic acid) (PAA) as the polyimide precursor via a direct ion-exchange self-metallization technique. The process has been clarified to involve the loading of silver(I) into PAA via ion exchange, the thermally induced reduction of silver(I) to silver(0) and the concomitant imidization of PAA to polyimide upon thermal treatment, the subsequent silver-catalyzed and oxygen-assisted decomposition of the polyimide overlayer, and the self-accelerated aggregation of silver clusters on the film surface to produce well-defined surface silver layers. By employing $[\text{Ag}(\text{NH}_3)_2]^+$ solution with a concentration of only 0.01 M and an ion-exchange time of no more than 10 min, the controlled formation of highly reflective and conductive silver surfaces upon thermal treatment at 300 °C for less than 4.5 h indicates that the present work provides an efficient route and an efficacious silver species for polyimide surface metallization. Although the alkaline characteristics of $[\text{Ag}(\text{NH}_3)_2]^+$ have a strong hydrolysis effect on the polyimide precursor chains, the final metallized films retain the key mechanical and thermal properties of the pure polyimide. Films were characterized by ATR-FTIR, XPS, ICP-AES, SEM, TEM, DSC, TGA, reflectivity, conductivity, and mechanical measurements.

1. Introduction

The characteristics of polyimide, including excellent mechanical strength, good thermal stability, high chemical resistance, and easy patterning, make it an important engineering material that could be used in many fields.^{1–6} Surface-silvered polyimide (PI) films, which combine the outstanding chemical and physical properties of the polyimide matrix and the excellent reflective and conductive properties of the surface silver layers, are widely attractive in the microelectronics and aerospace industries.^{7–10} Potential applications include flexible printed circuit boards (FPCBs),^{11,12} flexible conductive tape,¹³ magnetic data storage,^{12,14,15} highly active catalysts,^{15–18} optics,^{16,19–22} microelectronic devices,^{16,23,24} electromagnetic interference shielding filters,²⁵ and highly reflective thin film reflectors and concentrators in space environments for solar thermal propulsion or large-scale radiofrequency antennas for space applications.^{10,26–28}

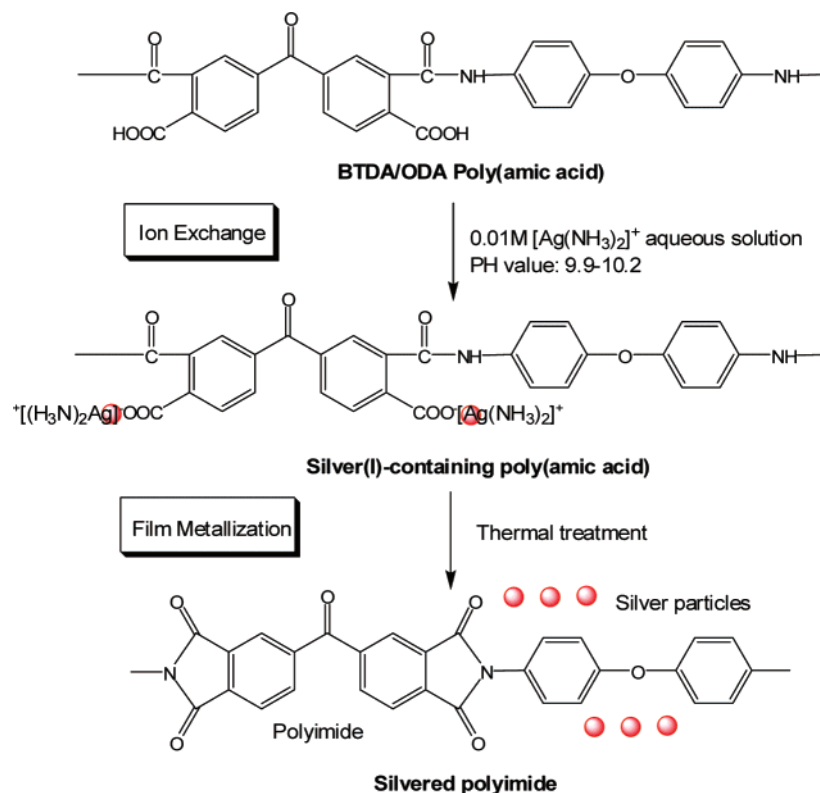
Several methods have been developed to produce surface-metallized polymeric films. One of the most well-established approaches is external deposition, which directly deposits a metal phase onto a previously prepared substrate.^{10,22,29,30} However, formation of surface silver layers on polyimide films with this method is unfeasible because silver is a passive metal and the films are usually prepared with very poorly adhered metallic layers.^{13,31}

As an alternative, in the 1990s, Southward's group reported an in situ single-stage self-metallization protocol that can also be conceptualized as inverse chemical vapor deposition.¹⁰ This

in situ method has been considered to be the most likely for preparing surface-silvered polyimide films because it has the advantages of processing simplicity and outstanding adhesion at the polymer–metal interface. For typical representative research works on this technique, see refs 10, 27, and 32–34. Highly reflective and electrically conductive surface-silvered polyimide films (maximum reflectivity, >97%; surface resistivity, <0.1 Ω/square) have been fabricated with this technique. However, successes were realized only when complex silver compounds with bridging β-diketonate ligands such as (1,1,1,5,5,5-hexafluoroacetylacetonato) silver(I) (AgHFA) and (1,1,1-trifluoroacetylacetonato) silver(I) (AgTFA)—which are usually very unstable, need to be freshly prepared, and are quite expensive—were used as the silver precursor.^{13,33} Nevertheless, metallization could be realized only on the air side of the film. Neither reflectivity nor conductivity was observed on the glass side. In addition, attempts to fabricate silvered polyimide films using simple silver salts have never achieved real success. In particular, films formed with silver nitrate are visually degraded and brittle without mechanical usefulness.^{33,35}

Because of the limitations of the above route, our group has developed a novel direct-ion-exchange self-metallization method aimed at fabricating surface-silvered polyimide films by employing simple silver compounds, especially silver nitrate, as the precursor. The approach works by introducing metal ions into pure poly(amic acid) (PAA), which contains many carboxylic acid groups (active components of an ion-exchange reaction), through ion exchange of the damp-dry PAA films in an aqueous silver(I) solution. Subsequent thermal treatment of the silver(I)-doped PAA films under tension converts the

* To whom correspondence should be addressed. Tel.: +86-10-6442-1693. Fax: +86-10-6442-1693. E-mail: wdz@mail.buct.edu.cn.

SCHEME 1: Ideal Synthetic Protocol for Producing Metallized BTDA/ODA Polyimide Films Using Silver Ammonia Complex Cation as the Precursor via the Direct Ion-Exchange Self-Metallization Process


precursor into its final polyimide form, with concomitant silver reduction and aggregation giving metallic layers on the polymer surfaces.^{36–38} This ion-exchange technique was demonstrated to be a rather effective approach for the metallization of polyimide films in our recent publications. In particular, double-surface-silvered polyimide films with high reflectivity and conductivity on both sides were fabricated. For the 3,3',4,4'-benzophenonetetracarboxylic acid dianhydride/4,4'-oxidianiline (BTDA/ODA-) based polyimide matrix, the silvered films were prepared with optimum reflectivities of 71% and 84% and surface resistances of 4.1 and 1.3 Ω /square on the upside and underside, respectively, when silver nitrate (AgNO_3) was employed as the silver source.³⁷ Similarly, by utilizing silver fluoride (AgF), maximum reflectivities higher than 80% and 100% and electrical resistances of less than 0.6 and 0.2 Ω /square on the upside and underside, respectively, were achieved.³⁸

In the present study, we report our efforts on the formation of silvered surfaces on BTDA/ODA-based polyimide films using silver ammonia complex cations ($[\text{Ag}(\text{NH}_3)_2]^+$) as the silver precursor via the direct ion-exchange self-metallization technique. The ideal synthetic protocol is shown in Scheme 1. This work was undertaken because the efficiencies of polyimide film metallization in previous works obtained by utilizing AgNO_3 and AgF as the silver precursor were not satisfactory. To fabricate the above two films, BTDA/ODA poly(amic acid) films were ion-exchanged in an aqueous 0.4 M AgNO_3 solution for 40 min and in an aqueous 0.1 M AgF solution (saturated concentration, 0.14 M) for 20 min, respectively.^{37,38} Moreover, the AgNO_3 -ion-exchanged film must be thermally treated at 300 $^\circ\text{C}$ for more than 9 h to achieve its optimum properties.³⁷ However, the experimental results obtained here using $[\text{Ag}(\text{NH}_3)_2]^+$ indicate that highly reflective and conductive silver layers were successfully fabricated on the polyimide film using more dilute silver(I) solution (0.01 M), a shorter ion-exchange time (no more than 10 min), and a shorter thermal treatment

time (less than 4.5 h at 300 $^\circ\text{C}$). Moreover, the final metallized films were prepared with well-boned surface silver layers and retained the key thermal and mechanical properties of the pure polyimide film. The mechanisms associated with the efficient formation of silver surfaces and the ion exchange between the alkaline $[\text{Ag}(\text{NH}_3)_2]^+$ and the PAA precursor films are discussed in detail. The surface, structural, and morphological characteristics of the resulting films were characterized by UV/vis spectrometry, surface reflectivity measurements, attenuated total reflection-Fourier transform infrared spectroscopy, X-ray diffraction, scanning electron microscopy, transmission electron microscopy, and X-ray photoelectron spectroscopy.

2. Experimental Section

2.1. Materials. 3,3',4,4'-Benzophenonetetracarboxylic dianhydride (BTDA) was purchased from Acros Organics and used without further purification. 4,4'-Oxidianiline (4,4'-ODA) was obtained from Shanghai Research Institute of Synthetic Resins and recrystallized from ethyl acetate prior to use. Dimethylacetamide (DMAc) (analytically pure, $\leq 0.1\%$ water) was purchased by Tianjin Fu Chen Chemicals Reagent Factory and used after distillation. Ammonia solution (analytically pure, 25–28 wt %) was purchased from Tianjin No. 3 Chemical Reagent Factory. Silver nitrate (AgNO_3) (analytically pure, $\geq 99.8\%$ content) was produced by Beijing Chemical Works and used as received. Silver ammonia complex cations ($[\text{Ag}(\text{NH}_3)_2]^+$) were easily prepared by adding dilute ammonia solution dropwise to the aqueous AgNO_3 solution until a transparent solution was obtained. In the present work, a 0.01 M aqueous $[\text{Ag}(\text{NH}_3)_2]^+$ solution with pH values of 9.9–10.2 was used.

2.2. Preparation of Metallized Films. The BTDA/ODA poly(amic acid) solution was prepared with a 1 mol % offset of dianhydride at 20 wt % solids in DMAc. The inherent viscosity of the synthesized resin was ca. 1.8 dL/g at 35 $^\circ\text{C}$. By

spreading the homogeneous poly(amic acid) solution onto a clean glass plate and allowing the solvent to evaporate, damp-dry poly(amic acid) films with thicknesses of 40–45 μm and DMAc contents in the range of 38.5–39.2 wt % were then produced. These films were next peeled from the glass substrate and treated in a 0.01 M aqueous $[\text{Ag}(\text{NH}_3)_2]^+$ solution to load silver ions into the matrix via ion exchange. For clarity, the surface of the damp-dry PAA film in contact with the glass substrate is referred to as the upside, and that exposed to the atmosphere is referred to as the underside. After being rinsed thoroughly with deionized water, the silver(I)-doped films were thermally treated under tension in a forced-air oven. The thermal cycles are heating over 1 h to 135 $^\circ\text{C}$ and holding for 1 h, heating to 300 $^\circ\text{C}$ over 2 h, and holding the temperature constant at 300 $^\circ\text{C}$. Thermal curing cycloimidizes the poly(amic acid) and simultaneously induces an internal silver reduction and then aggregation to form silver metallic layers, as depicted in Scheme 1.

2.3. Film Characterization. The amount of silver(I) loaded into the PAA films was quantified with a Seiko Instruments SPS 8000 inductively coupled plasma (ICP) atomic emission spectrometer. The measurements were performed after the silver-doped PAA films had been dissolved in a 5 wt % nitric acid solution.

Attenuated total reflection-Fourier transform infrared (ATR-FTIR) spectra of the films were collected using a Nicolet Nexus 670 IR spectrometer.

Reflectivity spectra (relative to a BaSO_4 mirror set at 100% reflectivity) were obtained on a Shimadzu 2501PC UV/vis spectrophotometer at an incidence angle of 8 $^\circ$ in the 200–800 nm wavelength range. The values at 531 nm were selected to represent the film's reflectance in the visible light region. Surface electrical resistivities were measured with a RTS-8 four-point probe meter produced by Guangzhou Semiconductor Material Research Institute in China.

The pH values of the aqueous solution were measured with a PHS-2C pH meter produced by Shanghai Kangyi Instrument Co., Ltd. (SHKY). The pH meter was calibrated using both aqueous phosphate mixture solution with a pH value of 6.86 and aqueous sodium tetraborate solution with a pH value of 9.18 prior to measurements.

Surface morphologies were recorded on a Hitachi S-4300 field-emission scanning electron microscope (FE-SEM) operating at 15 kV. The samples were coated with ca. 5 nm of platinum prior to the measurements.

The cross-sectional morphology of the films was observed using a Hitachi H-800 transmission electron microscope (TEM) at an accelerating voltage at 200 kV. Samples for TEM observations were prepared by adhering the film on a poly(vinyl chloride) plate and then cutting it perpendicular to the film surface using an ultramicrotome. These thin sections floating on a water bath were mounted onto the carbon-coated TEM copper grids.

X-ray diffraction (XRD) data were recorded on a D/Max2500VB2+/PC X-ray diffractometer (Rigaku, Tokyo, Japan) in the 5–90 $^\circ$ range at a scanning rate of 0.18 $^\circ/\text{s}$.

X-ray photoelectron spectroscopy (XPS) measurements were performed on an ESCALAB 250 spectrometer (Thermo Electron Corporation) equipped with a monochromatic Al K α X-ray source. The spectra were collected at a takeoff angle of 45 $^\circ$. The pressure in the analysis chamber was maintained at 2×10^{-10} mbar or lower during each measurement.

Differential scanning calorimetry (DSC) and thermal gravimetric analysis (TGA) were conducted on a NETZSCH STA

TABLE 1: XPS Surface Composition Data for the Poly(amic acid) Films Ion-Exchanged in 0.01 M Aqueous $[\text{Ag}(\text{NH}_3)_2]^+$ Solution for Varying Times^a

ion-exchange time (min)	relative atomic concentration (%)			
	C 1s	O 1s	N 1s	Ag 3d
0 (pure PAA)	70.27	24.39	5.34	0.00
5	50.37	18.52	22.23	8.88
10	44.71	18.26	26.25	10.78

^a Measurements were performed on the underside.

449C system at a heating rate of 5 K min $^{-1}$. Mechanical properties were evaluated using an Instron-1185 system.

3. Results and Discussion

3.1. Ion Exchange. Poly(amic acid)s have significantly higher cation-complexing properties than their imide forms, because of the presence of many active carboxylic acid groups in the macromolecules. This characteristic allows for in situ reactions with the salts of noble metals having labile anions to generate a metal–polymeric blends.¹⁶ In our recent publications,^{36–38} we demonstrated that silver ions can be successfully introduced into the poly(amic acid) films by ion exchange in aqueous silver(I) solutions, and we suggested that the metal ions were loaded through the coordination of the negatively charged polycarboxylate groups with the positive silver ions to form a silver polycarboxylate salt, silver polyamate, in the precursor films. However, as described earlier, the efficiencies of incorporating metal ions using silver nitrate³⁷ and silver fluoride³⁸ are rather disappointing, i.e., the silver(I) solution must have a high concentration and the necessary ion-exchange time is too long. Accordingly, an aqueous silver ammonia complex cation solution was employed in the present work. The ideal chemistry involved in the film preparation process, including ion exchange and film metallization, is depicted in Scheme 1. This alkaline silver cation was selected because we believe that its basic characteristics should accelerate the dissociation of carboxylic acid groups and consequently greatly promote their coupling with silver ions.

However, because of the presence of amide groups in the PAA macromolecules, the loading of silver via ion exchange is inevitably accompanied by the hydrolysis and degradation of the polymer chains, especially in alkaline environments. Thus, in the present study, a $[\text{Ag}(\text{NH}_3)_2]^+$ solution with a concentration of only 0.01 M (pH 9.9–10.2) was selected, and the ion-exchange time was confined to no more than 10 min. Nevertheless, as quantified by ICP atomic emission spectroscopy, the silver(I) loaded into the PAA films reached 6.59 and 7.23 wt % after only 5 and 10 min of treatment, which is significantly higher than the 4.32 wt % obtained for films that were ion-exchanged in a 0.4 M AgNO_3 solution for 40 min.³⁷ Correspondingly, the XPS composition data in Table 1 also indicate that the amount of silver ions on the PAA surfaces reached levels of 8.88 and 10.78 atom %, respectively. These results demonstrate that $[\text{Ag}(\text{NH}_3)_2]^+$ is indeed a rather effective silver source for ion exchange. Moreover, the rapid and highly efficient loading of silver(I) into the precursor films can reasonably be attributed to the alkaline nature of the $[\text{Ag}(\text{NH}_3)_2]^+$ solution, as mentioned previously.

The chemical state of the metal ions loaded into the precursor films is always one of the primary concerns. Figure 1 shows the ATR-FTIR characterization results of the PAA films before and after ion exchange. The appearance of a strong absorbance peak at 1361 cm^{-1} and the broadening of the band near 1599 cm^{-1} in the IR spectra of the films immersed in a 0.01 M

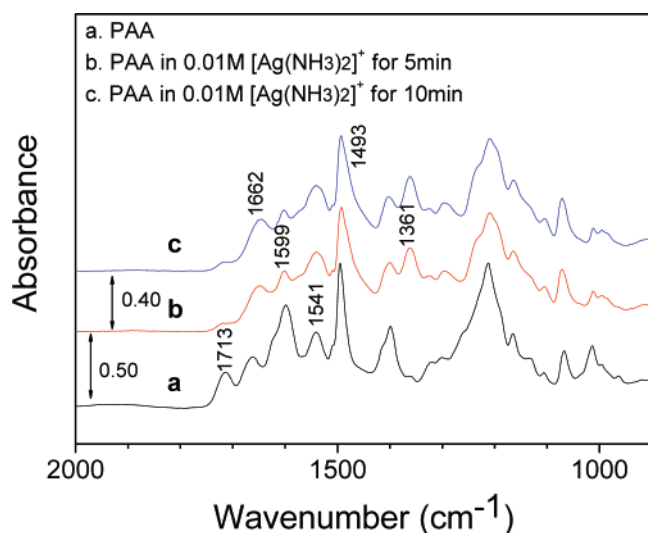


Figure 1. ATR FT-IR spectra of the metal-free pure poly(amic acid) film and the silver(I)-doped precursor films prepared with ion-exchange times of 5 and 10 min in 0.01 M $[\text{Ag}(\text{NH}_3)_2]^+$ solution.

aqueous silver ammonia complex cation solution for 5 min (Figure 1b) and 10 min (Figure 1c) indicate that metal polycarboxylate salts were successfully formed in the precursor films during the ion-exchange process.^{37,39–41} Initially, we expected that this was the result of the successful coordination of the silver ammonia complex cations with the carboxylic groups and that the silver(I) was present in the form of $[\text{Ag}(\text{NH}_3)_2]^+$ in the precursor films, as illustrated in Scheme 1. This is not an unreasonable conclusion because $[\text{Ag}(\text{NH}_3)_2]^+$ is a quite stable silver(I) species. However, XPS results entirely refuted this expectation. Figure 2 displays the XPS Ag 3d core-level spectra for the PAA films ion-exchanged in (a) 0.4 M AgNO_3 solution for 40 min, (b) 0.1 M AgF solution for 20 min, and (c) 0.01 M $[\text{Ag}(\text{NH}_3)_2]^+$ solution for 5 min. As for the first two films, the high-resolution spectrum for the alkaline-silver(I)-ion-exchanged film also gave Ag 3d signals at the same binding energy position of about 368.8 eV. This suggests that the chemical state of the loaded metal ions in the $[\text{Ag}(\text{NH}_3)_2]^+$ -PAA film is the same as that in the AgNO_3 and AgF films, i.e., the silver ions are mainly present in the form of silver polycarboxylate ($-\text{COO}^- \text{Ag}^+$ pairs).

In light of these results, the ion-exchange reactions in Scheme 1 must be reconsidered, and possible silver-loading mechanisms are proposed as in Scheme 2. It is suggested that the ammonia molecules are released from the silver complex (reaction 1) and subsequently interact with the carboxylic acid groups to generate ammonium carboxylate pairs ($-\text{COO}^- \text{NH}_4^+$) with better solubility in water and better ability to dissociate (reaction 2). Finally, the silver ions released from reaction 1 combine with the ammonium carboxylate pairs to load the silver ions through the formation of $-\text{COO}^- \text{Ag}^+$ pairs, as depicted in reaction 3. This silver-loading mechanism seems to be reasonable because the ion-exchange reaction between $-\text{COO}^- \text{NH}_4^+$ and Ag^+ is considered to be much faster than that between $-\text{COOH}$ and Ag^+ , which could logically account for the rapid and efficient loading of silver(I) into PAA using silver ammonia complex cation solution. In addition, the XPS data in Table 1 indicate that the surface atomic concentration of nitrogen (i.e., the N 1s signal) increased by a factor of 4–5 after ion exchange, supporting the occurrence of the above-suggested reactions, especially reaction 2.

Although allowing silver ions to be loaded efficiently, the utilization of $[\text{Ag}(\text{NH}_3)_2]^+$ to perform ion-exchange reactions

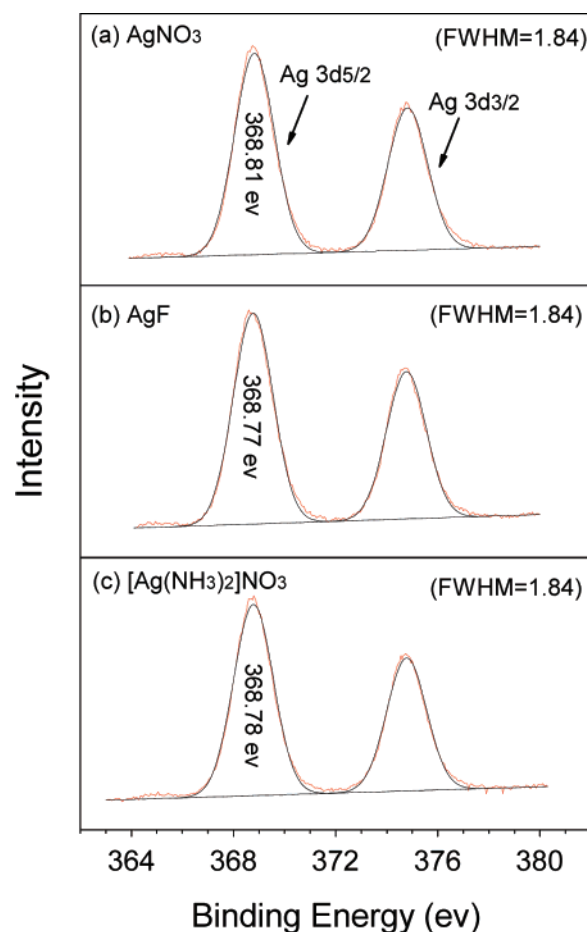
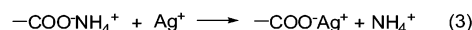
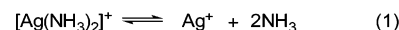


Figure 2. XPS Ag 3d core-level spectra for the PAA films ion-exchanged in (a) 0.4 M AgNO_3 solution for 40 min, (b) 0.1 M AgF solution for 20 min, and (c) 0.01 M $[\text{Ag}(\text{NH}_3)_2]^+$ solution for 5 min.

SCHEME 2: Possible Reaction Mechanism Suggested for the Loading of Silver Ions into PAA through Ion Exchange between Carboxylic Acid Groups and Silver Ammonia Complex Cations



Overall reaction:



with poly(amic acid) is risky because the alkaline nature of the silver ion solution would result in hydrolysis of the precursor films. The extensively increased nitrogen atomic concentrations (Table 1) after ion exchange might be direct evidence of this. However, it is fortunate that, under our present experimental conditions, no seriously destructive effect on the precursor films was observed. The remaining absorption peak at 1713 cm^{-1} attributed to the vibrational modes of the carboxylic acid and the bands at 1662 and 1541 cm^{-1} corresponding to the vibrational mode of the amide group, observed on the PAA films after ion exchange (Figure 1b,c), reflect the amic acid characteristics of the ion-exchanged film.^{42,43} The characteristic functional groups present in basic PAA molecules retained their integrity after being treated in the alkali silver solution.

3.2. Film Metallization. The ideal chemistry involved in the film metallization process is depicted in Scheme 1. Thermal curing converts the poly(amic acid) into its final polyimide form,

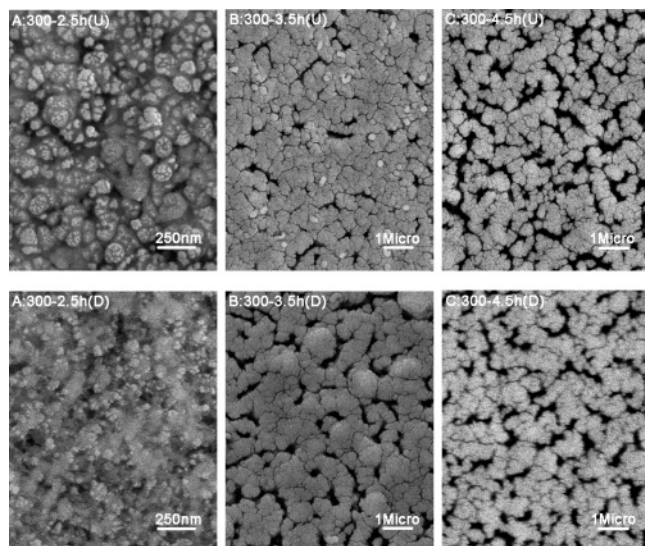


Figure 3. FE-SEM images of double-surface-silvered polyimide films with an ion-exchange time of 10 min in 0.01 M aqueous $[\text{Ag}(\text{NH}_3)_2]^+$ solution that were cured to 300 °C for (A) 2.5, (B) 3.5, and (C) 4.5 h. (U, upside of the film; D, underside of the film.)

with concomitant silver reduction and aggregation giving the silver–polyimide hybrid films. However, to obtain a flat and compact film characterized by good mechanical properties, it is necessary that the silver(I)-doped precursor be thermally treated under uniform tension. Otherwise, curl, shrinkage, or deformation would occur because of the thermoplastic characteristics of the poly(amic acid) molecules.

In our initial work, efforts to achieve surface metallization mainly focused on the films ion-exchanged in 0.01 M aqueous $[\text{Ag}(\text{NH}_3)_2]^+$ solution for 10 min. Figure 3A–C shows the surface topographies of the produced silver–polyimide composite films thermally treated to 300 °C for 2.5, 3.5, and 4.5 h, respectively. As can be clearly observed, well-established silver layers formed on both the upside and underside surfaces of the hybrid films, particularly after 3.5 h at 300 °C (Figure 3B,C). This suggests that surface silver metallization on the polyimide matrix was successfully achieved using silver ammonia complex cation as the silver source via the direct ion-exchange self-metallization process.

Reflectivity measurements were performed on both the upside and underside surfaces of the metallized films cured at different stages of the thermal cycle. Figure 4A shows plots of reflectivity versus cure time/temperature for the 10-min ion-exchanged hybrid films. It is exciting to note that maximum reflectivities of 80.5% and 91.0% were achieved on the upside and underside, respectively, of the metallized films that were thermally treated for 4.5 h at 300 °C (Figure 3C). The variation of surface electrical resistivity for the hybrid films with increasing cure time/temperature is also reported in Table 2. For thermal treatments of less than 300 °C for 1 h, the characterization data indicate that conductivity was never achieved on either side of the metallized films. However, films were soon fabricated with surface resistance values of 3.2 and 7.0 Ω/square on the upside and underside, respectively, after only an additional 1 h of thermal treatment on the 10-min-ion-exchanged films (300 °C for 2 h), implying the formation of very conductive surfaces. As the thermal cure proceeds, the surface resistivity rapidly decreased to less than 1 Ω/square , and for treatment at 300 °C for 4.5 h, metallized films with surface electrical resistances of 0.6 and 0.8 Ω/square on the upside and underside, respectively, were produced. Both the reflectance and resistance characteriza-

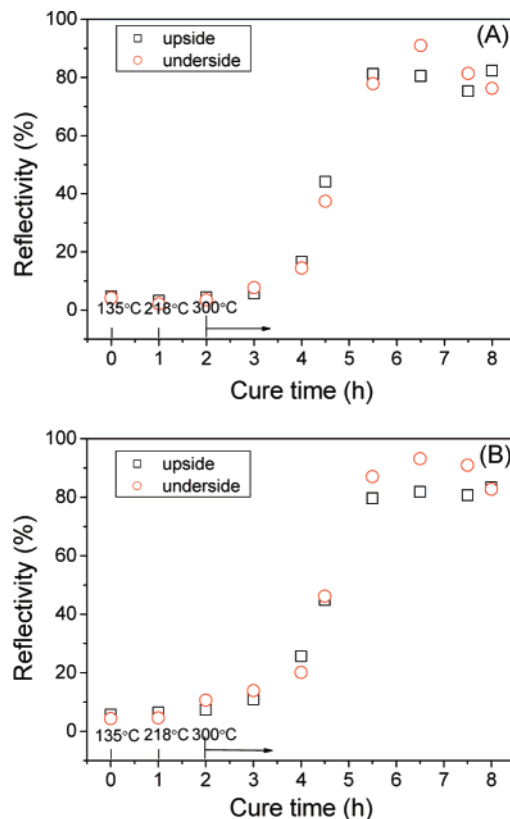


Figure 4. Development of reflectivity on the upside and underside surfaces as a function of the cure protocol for the hybrid films ion-exchanged for (A) 10 and (B) 5 min in a 0.01 M aqueous $[\text{Ag}(\text{NH}_3)_2]^+$ solution. (Time zero is curing at 135 °C for 1 h.)

TABLE 2: Surface Resistivity Data (Ω/square) for the 10- and 5-min-Ion-Exchanged BTDA/ODA Films Cured to 300 °C for Varying Times

thermal history	10-min-ion-exchanged		5 min-ion-exchanged	
	upside	underside	upside	underside
300 °C for 1 h	>10 ⁶	>10 ⁶	>10 ⁶	>10 ⁶
300 °C for 2 h	3.2	7.0	6.0	5.5
300 °C for 2.5 h	2.0	4.5	1.7	0.7
300 °C for 3.5 h	0.8	0.7	0.7	0.4
300 °C for 4.5 h	0.6	0.8	0.6	0.6
300 °C for 5.5 h	0.8	0.6	0.4	0.4

tion results indicate that the silver layers formed on the film surfaces are highly reflective and conductive, the characteristics that are the most important targets of our work.

Success was also achieved in our later work by shortening the ion-exchange time in 0.01 M $[\text{Ag}(\text{NH}_3)_2]^+$ solution to 5 min. With maximum reflectivities of 81.8% and 93.1% and surface resistances of 0.6 and 0.6 Ω/square on the upside and underside, respectively, after being cured to 300 °C for 4.5 h, the 5 min-ion-exchanged films also were well-metallized on both sides with high reflectivity and conductivity, as indicated in Figure 4B and Table 2. Compared to the BTDA/ODA– AgNO_3 silvered films³⁷ (optimum reflectivities of 71% and 84%, surface resistances of 4.1 and 1.3 Ω/square) prepared with an ion-exchange time of 40 min in 0.4 M aqueous AgNO_3 solution and cured to 300 °C for 9 h, the successful formation of silvered surfaces with such desirable reflective and conductive properties on both sides by employing a 0.01 M silver(I) solution with an ion-exchange time of merely 10 or 5 min and a thermal treatment time of only 4.5 h at 300 °C strongly suggests that silver ammonia complex cation is a rather effective silver species for polyimide film metallization.

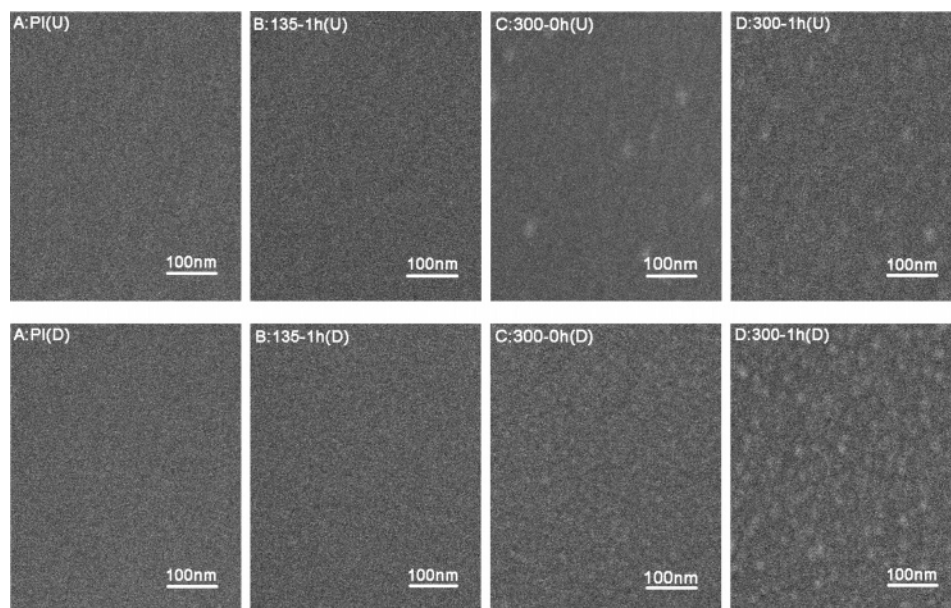


Figure 5. FE-SEM images of the upside and underside surfaces of (A) the pure polyimide film and (B–D) the 10-min-ion-exchanged hybrid films cured to (B) 135 °C for 1 h, (C) 300 °C for 0 h, and (D) 300 °C for 1 h. (U, upside of the film; D, underside of the film.)

Nevertheless, the plots in Figure 4 indicate that the surface properties of the metallized films develop gradually with increasing cure time and temperature in a stepwise manner. For thermal treatments of less than 300 °C for 1 h, both the upside and underside of the hybrid films exhibited rather disappointing reflectivities in the range of 3–8% (Figure 4A), which are not much different from the ca. 6% reflective surfaces of pure polyimide films. A rapid increase in reflectivity began for a thermal treatment of 300 °C for 2 h, and in no more than 2 h, highly reflective surfaces were achieved. For the same time treatment (300 °C for 2 h), the films prepared were also conductive, as shown in Table 2, and the surface resistances rapidly decreased to less than 1 Ω /square with increasing cure time. Further thermal treatment at 300 °C did not improve the reflectivity and conductivity significantly, but seemed to be necessary to achieve the optimum surface properties.

SEM micrographs, reflecting the variation of the surface morphologies of the 10-min-ion-exchanged hybrid films subjected to thermal treatments of less than 300 °C for 1 h, are shown in Figure 5. As a reference, SEM analysis was also performed on the pure polyimide films (Figure 5A). After being heated at 135 °C for 1 h, the films exhibited almost the same completely transparent light-yellow appearance as the pure BTDA/ODA precursor films. The SEM images in Figure 5B show two rather plain surfaces without the detection of any silver particles. Also, the X-ray diffraction pattern in Figure 6 for the films subjected to a thermal treatment of 135 °C for 1 h exhibits no reflections expected for the reduced silver metal, consistent with the low reflectivities observed for this time and temperature. In contrast, the XRD patterns soon gave very distinct peaks characteristic of the crystalline state of face-centered-cubic (fcc) silver metal after the temperature was raised to 218 °C. Simultaneously, the silver(I)-doped films turned dark blue/black and became completely nontransparent, which would most likely correspond to silver(I) reduction and subsequent aggregation in the polymer matrix. Further thermal treatment converts the films to blue at 300 °C and next to green after thermal treatment at 300 °C for 1 h.

The frequent color changes at this thermal stage are suggested to originate from the continuous aggregation of the reduced silver atoms to form larger silver particles. However, the main

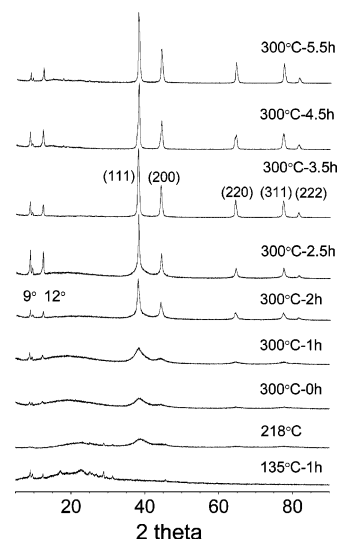


Figure 6. XRD patterns of the silvered polyimide films after thermal treatments of different times/temperatures.

XRD peak in the silver (111) region did not narrow significantly with increasing cure time and temperature, suggesting a rather slow increase in the dimension of the silver particles upon thermal treatments of less than 300 °C for 1 h. The SEM images in Figure 5C,D also demonstrate the reduction of silver(I) and aggregation of silver atoms at the film surfaces. Many small spherical silver particles with diameters on the order of ~20 nm or less were uniformly distributed on the film surfaces, especially for the films cured to 300 °C for 1 h (Figure 5D). Yet, these small aggregates were all island-like and separated from each other, consistent with the lack of conductivity at this point. However, with reflectivities of only 5.7% and 7.7% on the upside and underside, respectively (Figure 4A), the films remained at a very low reflective level.

XPS measurements (with a probing depth of about 5–7.5 nm) were performed on the metallized films. As reported in Table 3, the film subjected to a thermal treatment of 300 °C for 1 h displays a surface silver atomic concentration of only 3.94%, whereas its carbon atomic content is approximately 66%, close to that of the pure polyimide, indicating that the surface

TABLE 3: XPS Surface Composition Data for the 10-min-Ion-Exchanged Hybrid Films Cured at Different Thermal Stages^a

film sample	relative atomic concentration (%)			
	C 1s	O 1s	N 1s	Ag 3d
pristine PI, 300 °C for 5 h	74.32	21.59	4.09	0.00
PI–Ag, 300 °C for 1 h	65.99	17.91	12.16	3.94
PI–Ag, 300 °C for 2.5 h	57.67	17.23	15.87	9.23
PI–Ag, 300 °C for 4.5 h	35.52	24.19	16.10	24.18

^a Measurements were performed on the underside.

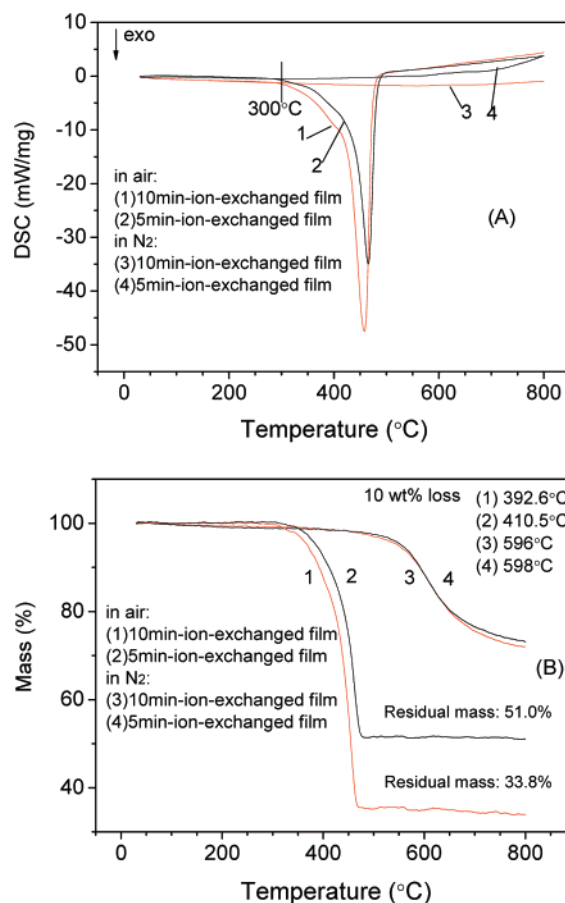
TABLE 4: Thermal and Mechanical Properties of the Silvered Polyimide Films

film sample	ion-exchange time (min)	tensile strength (MPa)	modulus (MPa)	percent elongation	10%-weight-loss temperature (°C)	
					in N ₂	in air
pure PI at 300 °C for 5 h	0	137.6	2932.5	14.7	565	571
PI–Ag at 300 °C for 4.5 h	5	110.7	3018.2	8.6	598	411
PI–Ag at 300 °C for 4.5 h	10	102.8	3193.6	6.3	596	393

of the metallized films is dominated by the organic species. Thus, the observation of very poor reflectivities on hybrid film surfaces with so many attached silver particles (Figure 5D) is reasonable because the coverage of a thin polymer overlayer that strongly absorbs in the visible light regions on the top film surfaces would greatly compromise the reflective features of the silver particles aggregated on the surfaces.

However, one initially confusing aspect is that the surface atomic concentrations indicated by the silver 3d peaks, and also the N 1s peaks, of the hybrid films substantially decreased after thermal treatment, relative to those of the silver(I)–PAA precursor films. As shown in Table 1, after ion exchange in a 0.01 M aqueous [Ag(NH₃)₂]⁺ solution for 10 min, the PAA film had a surface elemental composition of 10.78 atom % Ag, 26.25 atom % N, and 44.71 atom % C. Compared to the pure PAA films (Table 1), the decreased C concentration and the increased N content on the silver(I)–PAA surface can be ascribed to the occurrence of PAA hydrolysis during ion exchange and the reaction of carboxylic acid groups with ammonia molecules introducing a large number of carboxylic ammonium (–COO[–]NH₄⁺) pairs into the macromolecule chains. In contrast, upon thermal treatment, the Ag and N atomic concentrations decreased to 3.94 and 12.16 atom %, respectively, with a concomitant increase in the C atomic content to approximately 66 atom %, as listed in Table 4 for the film subjected to a thermal treatment of 300 °C for 1 h. It is probable that the process of thermal cyclimidization of the silver(I)-doped PAA film to generate the polyimide matrix involves the decomposition of the carboxylic ammonium (–COO[–]NH₄⁺) components, which would possibly eliminate the nitrogen element by releasing free ammonia molecules from the system and regenerating the carboxylic acid groups (–COOH). In contrast, the concentration of Ag on the film surface following thermal treatment probably decreases because the movements of the polymer segments are more dynamic and much easier than those of the as-aggregated silver particles near the surface layer, especially at early stages of the thermal cycle where the cure temperature is not very high, so that a thin polymer overlayer is generated on the top surface. As a result, the C 1s peak becomes predominant, and the atomic contents of Ag and N are lowered.

Upon further thermal treatment of the film to 300 °C for 2.5 h, the XPS data in Table 3 show a sharp increase in the silver

**Figure 7.** (A) DSC and (B) TG analyses of the silvered polyimide films cured at 300 °C for 4.5 h.

concentration from 3.94 to 9.23 atom %, accompanied by a decrease in the carbon content from 65.99 to 57.67 atom %, indicating a discernible decomposition of the surface polymer overlayer. A rapid increase in reflectivity was observed near this point, and simultaneously, surface conductivity was obtained, as reported in Figure 4 and in Table 2. SEM micrographs in Figure 3A for the film cured to 300 °C for 2.5 h display completely different topographies from that of the prematurely cured films in Figure 5. Many larger silver particles were exposed and blended with the polymer frameworks on the film surfaces, which might account for the increased reflectivity and the conductivity. However, the fabrication of metallized films with such good electrical conductivities at such an early stage (300 °C for 2 or 2.5 h) is amazing, especially when the reflectivity was still at such a low level, because the appearance of electrical conductivity usually occurs after the achievement of high reflectivity and after a long thermal treatment time, as reported in the literature.^{13,33,37} Southward and Thompson³² suggested that the formation of conductive surfaces arises from the degradation of the intervening polymers between the metal particles to allow them to come into contact with each other. In the present system, although the ion-exchanged PAA films were successfully converted into the imide form after curing (as demonstrated by IR spectroscopy, not shown), it is reasonable that the polyimide structure might not be perfectly attained because of the ammonia-catalyzed hydrolysis of PAA chains occurring during ion exchange. Correspondingly, the formed polyimide is relatively easier to degrade, resulting in conductive films after shorter thermal treatment times.

A layer of faint whitish substance began to be appear on the metallized film surfaces after treatment at 300 °C for 3.5 h,

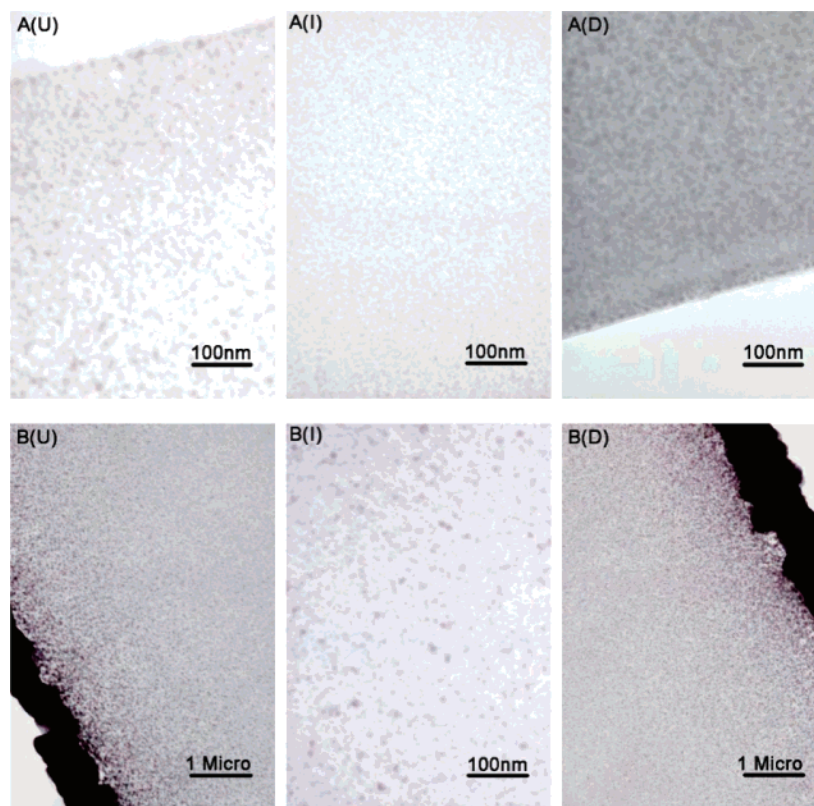


Figure 8. Cross-sectional TEM images of 10-min-ion-exchanged hybrid films cured at 300 °C for (A) 1 and (B) 4.5 h. (U, upside; I, interior; D, underside.)

and it became appreciable after an additional 1 h of thermal treatment. This whitish substance was undoubtedly derived from the degradation of surface polyimide layer induced by the thermal catalytic effects of the silver agglomerations deposited on the surface. XPS data shown in Table 3 for the film cured at 300 °C for 4.5 h give a surface silver content as high as 24.18 atom % and a carbon concentration as low as 35.52 atom %, confirming the occurrence of polymer decomposition. Meanwhile, the optimum film, with reflectivities of 80.5% and 91.0% and surface resistances of 0.6 and 0.8 Ω /square for the upside and underside, respectively, was obtained for the 10-min-ion-exchanged system. The SEM images in Figure 3B,C indicate that continuous and integrated silver layers formed on both sides of the metallized films.

In accordance with the wide variations of the film surface morphology in this final thermal stage, the XRD patterns in Figure 6 show that the full width at half-maximum of the strongest characteristic (111) reflection narrowed rather quickly after treatment at 300 °C for 2 h and the five reflections for the fcc silver crystallites became increasingly distinct, indicating the occurrence of dramatic silver aggregation and the subsequent formation of larger and more perfect silver crystallites. However, it is strange that two unexpected peaks appeared in the XRD patterns at about 9° and 12° for the films cured at 300 °C for 1 h or longer. Moreover, these peaks increased in intensity with increasing cure time up to 2.5 h, after which they receded again. It is presumed that these two unknown peaks can be attributed to the restricted silver aggregation in the present silver–polymer blend system producing imperfect, particularly porous silver crystallites. However, this interpretation cannot be confirmed with the available evidence, and further investigations are needed.

DSC analysis was also performed on the hybrid films, and the results are shown in Figure 7A. As can be observed, a strong

exothermic peak appears in the range of 300–500 °C for the metallized film measured under an air atmosphere (Figure 7A-1 and -2). The significant amount of heat released here is suggested to arise from the aggregation of unstable silver clusters, which had a high surface free energy and readily combined together to form larger thermodynamically stable aggregations. The stronger peak in Figure 7A-2 is due to the higher silver concentration in the 10-min-ion-exchanged hybrid film. However, in nitrogen environment, no pronounced thermal effect was observed in the present experimental temperature range (Figure 7A-3 and -4). These results indicate that silver aggregation is an oxygen-assisted process.

Along with the liberation of heat, a significant mass loss began to be observed in the TGA curves measured in air atmosphere, as shown in Figure 7B-1 and -2. Thus, the function of oxygen here should be that it helps to decompose the polymer constituent at the surface, thereby encouraging the aggregation of the small silver particles. However, once the silver aggregation is initiated, it becomes almost uncontrollable because the released heat would accelerate further aggregation of the silver particles following a chain-reacting mechanism. Enormous variations in the film surface morphology then resulted, and soon, well-defined silver layers with desirable surface performances were formed, as observed in Figure 3. Cross-sectional TEM also indicated the rapid formation of surface metal layers upon silver aggregation, as shown in Figure 8. For thermal treatment at 300 °C for 1 h (Figure 8A), the hybrid film was metallized with only negligible silver layers on the film surfaces. However, in no more than 4 h, near-perfect thin silver layers formed on each film side, as shown in Figure 8B for the film cured at 300 °C for 4.5 h. Therefore, we conclude that the formation of highly reflective and conductive silver layers on polyimide film is a result of the silver-catalyzed and oxygen-

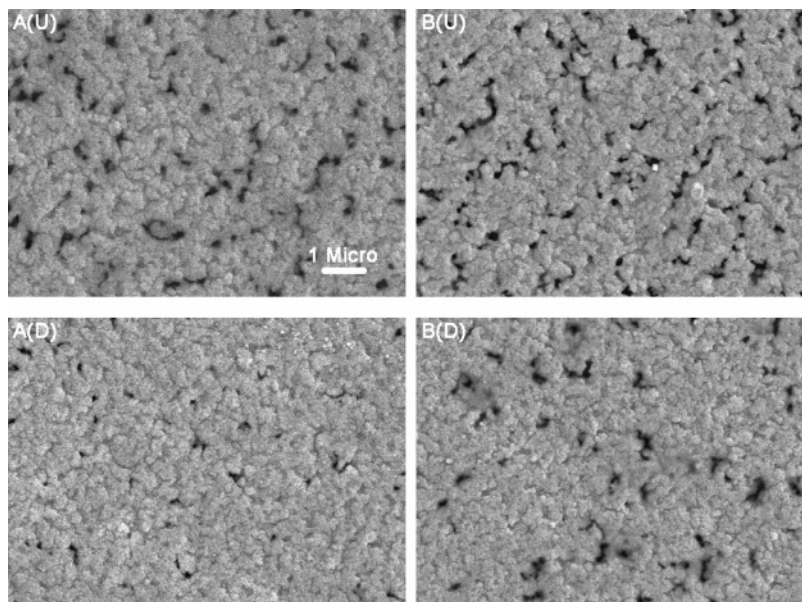


Figure 9. FE-SEM micrographs recorded for the upside and underside surfaces of the silvered polyimide films (A) before and (B) after the adhesion test. The film was initially ion-exchanged in 0.01 M $[\text{Ag}(\text{NH}_3)_2]^+$ for 5 min and then cured to 300 °C for 4.5 h. (U, upside of the film; D, underside of the film.)

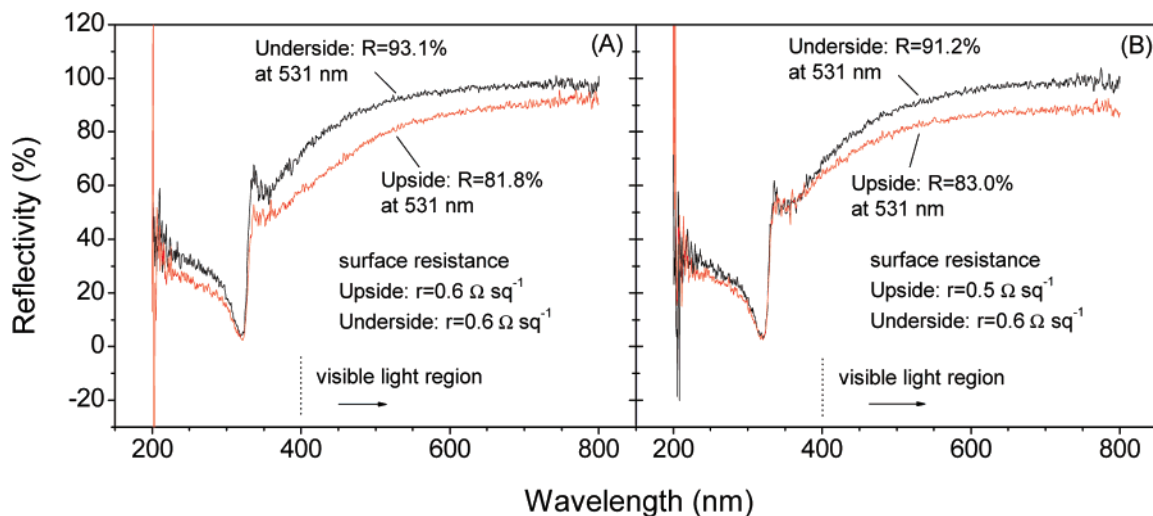


Figure 10. Specular reflectance spectra as a function of light wavelength in the range of 200–800 nm recorded for the upside and underside surfaces of the same film as in Figure 9 (A) before and (B) after the adhesion test.

assisted decomposition of the polymer overlayer and the self-accelerated aggregation of silver clusters on the film surface.

TEM images in Figure 8B also suggest that our hybrid films were fabricated with a sandwich structure, in which the silver is mainly concentrated in the near-surface layer. This is very favorable because the few metal particles remaining in the inner polymer bulk with very small sizes (~ 10 nm or less) make it possible for the metallized films to retain the key mechanical properties of the pristine polyimide, as shown later.

3.3. Adhesion Test. The adhesion between the metal layer and the underlying polymer substrate is always a primary concern when surface metallization is studied. As a qualitative evaluation, mechanical debonding studies were performed on the metallized films using commercial transparent adhesive tape. After the film had been fixed on a substrate, the sample was tested using 6-mm-wide adhesive tape by sticking it on the film surface and then peeling it off. Macroscopic observation indicated that no delamination occurred on either the upside or the underside surface after debonding. For further validation, SEM analysis was carried out on the metallized film before and

after the adhesion test, as shown in Figure 9. The fact that some metal agglomerates were drawn away from the silvered surfaces, as indicated by the peeling spots presented on the tested surfaces (Figure 9B), cannot be ignored. However, the overall morphologies before and after the peeling test were not distinctly altered. Continuous and net-like silver surfaces were still maintained. Furthermore, the surface reflectance and resistance features remained almost identical before and after adhesion test, as shown in Figure 10. Thus, it can be concluded that the adhesion at the silver–polyimide interface is quite acceptable for films prepared using $[\text{Ag}(\text{NH}_3)_2]^+$ via the direct ion-exchange self-metallization process. Here, the good bonding strength is attributed to the mechanical interlocking effect between silver and polyimide, as reported in the literature.^{10,12,32}

3.4. Mechanical and Thermal Characterization. As mentioned previously, the use of $[\text{Ag}(\text{NH}_3)_2]^+$ is risky, because the PAA chains might be seriously hydrolyzed by the alkaline silver-(I) solution during ion exchange, thereby giving metallized films with substantially degraded mechanical properties. This is true but only to a limited extent in the present work. Table 4 displays

the mechanical characterization data for the metallized films. As can be seen, the tensile strength of the polyimide film indeed decreased (by about 25–35 MPa) after metallization, especially for the 10-min-ion-exchanged films. However, the tensile strength still remains at a level higher than 100 MPa, and the modulus appears not to be diminished. Thus, it is confirmed that the key mechanical properties of the pure polyimide are retained, as previously anticipated from the TEM observations in Figure 8B.

The thermal data listed in Table 4 suggest that the thermal stability of the silver-doped films, as characterized by the temperature at which 10% weight loss occurred, was never lowered in a nitrogen environment. However, in air, the degradation temperatures were considerably lower than those of the host polyimide films. Such behavior is expected because silver particles have strong catalytic and oxidative degradation effects on the polymeric matrix, as reported in many publications.^{13,18} However, the respective decreases of about 160 and 180 °C for the 5- and 10-min-ion-exchanged hybrid films are somewhat larger than those for the AgNO₃ analogues (~130 °C lower than the pristine film), which might also be ascribed to the destructive effects of the alkaline silver(I) ions on the polymer matrix. In summary, although the bulk polyimide films were compromised after silver metallization, the remaining mechanical and thermal properties were still more than adequate for most purposes.

4. Conclusions

Our present work demonstrates that silvered surfaces with acceptable adhesion strength can be readily formed on the BTDA/ODA-based polyimide matrix using [Ag(NH₃)₂]⁺ as the silver precursor via the direct ion-exchange self-metallization technique. With an ion-exchange time of no more than 10 min in a 0.01 M [Ag(NH₃)₂]⁺ solution and with a thermal treatment time of only 4.5 h at 300 °C, silver–polyimide hybrid films were prepared with optimum surface reflectivities higher than 80% and 90% and electrical resistances of less than 0.6 and 0.8 Ω/square on the upside and underside, respectively, indicating the high efficiency of [Ag(NH₃)₂]⁺ for polyimide film metallization. Rather than direct loading of the [Ag(NH₃)₂]⁺ cations into the poly(amic acid) film via ion exchange, it was found that the incorporation of silver(I) species in the present system involves the formation of –COO[–]NH₄⁺ components and their subsequent reaction with silver ions (Ag⁺) to form the silver polyamate. Because of the pronounced hydrolysis of the precursor films induced by the alkaline nature of the [Ag(NH₃)₂]⁺ solutions during ion exchange, the mechanical and thermal properties of the final metallized films were considerably compromised; however, they could still satisfy the requirements for many practical applications.

Acknowledgment. The authors acknowledge financial support from the National Natural Science Foundation of China (NSFC, Project 50573007) and the program for New Century Excellent Talents in University (NCET-040118).

References and Notes

(1) Chen, Y. W.; Wang, W. C.; Yu, W. H.; Kang, E. T.; Neoh, K. G.; Vora, R. H.; Ong, C. K.; Chen, L. F. *J. Mater. Chem.* **2004**, *14*, 1406.

- (2) Fu, G. D.; Wang, W. C.; Li, S.; Kang, E. T.; Neoh, K. G.; Tseng, W. T.; Liaw, D. J. *J. Mater. Chem.* **2003**, *13*, 2150.
- (3) Liaw, D.-J.; Hsu, P.-N.; Chen, W.-H.; Lin, S.-L. *Macromolecules* **2002**, *35*, 4669.
- (4) Ranucci, E.; Sandgren, A.; Andronova, N.; Albertsson, A.-C. *J. Appl. Polym. Sci.* **2001**, *82*, 1971.
- (5) Wu, Z.; Wu, D.; Yang, W.; Jin, R. *J. Mater. Chem.* **2006**, *16*, 310.
- (6) Xiao, Y.; Chung, T.-S.; Chng, M. L. *Langmuir* **2004**, *20*, 8230.
- (7) Rubira, A. F.; Rancourt, J. D.; Taylor, L. T. In *Metal-Containing Polymeric Materials*; Carraher, C. E., Jr., Culbertson, B. M., Pittman, C. U., Jr., Sheats, J. E., Zeldin, M., Eds.; Springer: New York, 1996; p 357.
- (8) Rubira, A. F.; Rancourt, J. D.; Taylor, L. T.; Stoakley, D. M.; Clair, A. K. S. *J. Macromol. Sci.: Pure Appl. Chem.* **1998**, *A35* (4), 621.
- (9) Sawada, T.; Ando, S. *Chem. Mater.* **1998**, *10*, 3368.
- (10) Southward, R. E.; Stoakley, D. M. *Prog. Org. Coat.* **2001**, *41*, 99.
- (11) Ektessabi, A. M.; Hakamata, S. *Thin Solid Films* **2000**, *377–378*, 621.
- (12) Akamatsu, K.; Ikeda, S.; Nawafune, H. *Langmuir* **2003**, *19*, 10366.
- (13) Southward, R. E.; Thompson, D. S.; Thompson, D. W.; Clair, A. K. S. *Chem. Mater.* **1999**, *11*, 501.
- (14) Akamatsu, K.; Shinkai, H.; Ikeda, S.; Adachi, S.; Nawafune, H.; Tomita, S. *J. Am. Chem. Soc.* **2005**, *127*, 7980.
- (15) Huang, J.-c.; Qian, X.-f.; Yin, J.; Zhu, Z.-k.; Xu, H.-j. *Mater. Chem. Phys.* **2001**, *69*, 172.
- (16) Andreescu, D.; Wanekaya, A. K.; Sadik, O. A.; Wang, J. *Langmuir* **2005**, *21*, 6891.
- (17) Li, Y.; Lu, Q.; Qian, X.; Zhu, Z.; Yin, J. *J. Appl. Surf. Sci.* **2004**, *233*, 299.
- (18) Zhang, F.; Guan, N.; Li, Y.; Zhang, X.; Chen, J.; Zeng, H. *Langmuir* **2003**, *19*, 8230.
- (19) Akamatsu, K.; Ikeda, S.; Nawafune, H.; Deki, S. *Chem. Mater.* **2003**, *15*, 2488.
- (20) Beecroft, L. L.; Ober, C. K. *Chem. Mater.* **1997**, *9*, 1302.
- (21) Yen, C.-T.; Chen, W.-C. *Macromolecules* **2003**, *36*, 3315.
- (22) Rifai, S.; Breen, C. A.; Solis, D. J.; Swager, T. M. *Chem. Mater.* **2006**, *18*, 21.
- (23) Akamatsu, K.; Ikeda, S.; Nawafune, H.; Yanagimoto, H. *J. Am. Chem. Soc.* **2004**, *126*, 10822.
- (24) Kariuki, N. N.; Luo, J.; Hassan, S. A.; Lim, I.-I. S.; Wang, L.; Zhong, C. *J. Chem. Mater.* **2006**, *18*, 123.
- (25) Tachibana, Y.; Kusunoki, K.; Watanabe, T.; Hashimoto, K.; Ohsaki, H. *Thin Solid Films* **2003**, *442*, 212.
- (26) Bai, Z.; Chen, M. Y.; Tan, S. C. *Polym. Prepr.* **2002**, *43*, 1277.
- (27) Southward, R. E.; Thompson, D. W. *Mater. Des.* **2001**, *22*, 565.
- (28) Warner, J. D.; Pevzner, M.; Dean, C. J.; Kranbuehl, D. E.; Scott, J. L.; Broadwater, S. T.; Thompson, D. W.; Southward, R. E. *J. Mater. Chem.* **2003**, *13* (7), 1847.
- (29) Tian, M.; Wang, J.; Kurtz, J.; Mallouk, T. E.; Chan, M. H. W. *Nano Lett.* **2003**, *3* (7), 919.
- (30) Ward, L. J.; Schofield, W. C. E.; Badyal, J. P. S. *Chem. Mater.* **2003**, *15*, 1466.
- (31) Strunskus, T.; Grunze, M.; Kochendoerfer, G.; Woll, C. *Langmuir* **1996**, *12*, 2712.
- (32) Southward, R. E.; Thompson, D. W. *Adv. Mater.* **1999**, *11* (12), 1043.
- (33) Southward, R. E.; Thompson, D. W. *Chem. Mater.* **2004**, *16*, 1277.
- (34) Qi, S.-L.; Wu, D.-Z.; Wu, Z.-P.; Wang, W.-C.; Jin, R.-G. *Polymer* **2006**, *47*, 3150.
- (35) Southward, R. E.; Thompson, D. S.; Thompson, D. W.; Caplan, M. L.; Clair, A. K. S. *Chem. Mater.* **1995**, *7*, 2171.
- (36) Qi, S.; Wu, D.; Bai, Z.; Wu, Z.; Yang, W.; Jin, R. *Macromol. Rapid Commun.* **2006**, *27*, 372.
- (37) Qi, S.; Wu, Z.; Wu, D.; Wang, W.; Jin, R. *Chem. Mater.* **2007**, *19* (3), 393.
- (38) Qi, S.; Wu, Z.; Wu, D.; Wang, W.; Jin, R. *Langmuir* **2007**, *23* (9), 4878.
- (39) Lee, K.-W.; Kowalczyk, S. P.; Shaw, J. M. *Macromolecules* **1990**, *23*, 2097.
- (40) Okumura, H.; Takahagi, T.; Nagai, N.; Shingubara, S. *J. Polym. Sci. B: Polym. Phys.* **2003**, *41*, 2071.
- (41) Thomas, R. R.; Buchwalter, S. L.; Buchwalter, L. P.; Chao, T. H. *Macromolecules* **1992**, *25*, 4559.
- (42) Lee, K.-W.; Kowalczyk, S. P.; Shaw, J. M. *Langmuir* **1991**, *7*, 2450.
- (43) Pramoda, K. P.; Liu, S.; Chung, T.-S. *Macromol. Mater. Eng.* **2002**, *287*, 931.